# Mirror Coatings with Atomic Layer Deposition: Initial Results

Frank Greer*, Shouleh Nikzad, and Wesley Traub
Jet Propulsion Laboratory, California Institute of Technology,
4800 Oak Grove Dr., Pasadena, CA, USA 91109

## ABSTRACT

The new technology of Atomic Layer Deposition (ALD) holds promise to enable a future strategic mission that can address both ultraviolet (UV) astrophysics and optical exoplanet science with a shared telescope. The technology path to a shared telescope requires the development of a mirror coating with high reflectance from 100 nm to 1000 nm, and low polarization effects (i.e., s-p phase shifts that can vary with angle of incidence across a primary and secondary mirror) in the optical range. Currently, UV coatings have low reflectance, and conventional optical coatings have poor polarization properties for high-contrast coronagraph applications. In this paper we attempt to take a first step toward solving both problems simultaneously by using ALD, taking advantage of the fact that ALD can potentially produce mirror coatings with denser layers than conventional coatings (hence better reflectance, durability, and water resistance). In addition, ALD can potentially produce coatings with new composite materials (hence better control of polarization). We report here the results of our initial experiments with mirror coatings using ALD.

**Keywords:** atomic layer deposition, coatings, ultraviolet, visible, phase shift

## 1. INTRODUCTION

Exoplanet scientists have joined with ultraviolet astronomy scientists to study the potential of a single space mission that could serve both communities. The common point of interest is a single telescope with a split focal plane, sending the ultraviolet (UV) light to one set of instruments, and the visible light to a set of exoplanet imagers and spectrometers.

This concept works whether the exoplanet instrumentation is based on an external occulter or an internal coronagraph. In both cases the primary mirror (PM) and secondary mirror (SM) must have good reflectivity in the UV as well as in the visible. If an internal coronagraph is used, then there is an additional requirement on the visible coatings that they must have good spatial uniformity of reflectivity and also a small net phase shift between polarization components that are perpendicular to the plane of incidence (s-polarization) and parallel (p-polarization) over a broad spectral range.

The programmatic motivation for joining UV and exoplanets in a single space mission is that the cost of a mission, per community served, would then be nearly half of the total, since the major cost elements, the telescope, spacecraft, and launch vehicle would be shared. This is a powerful motivation in a fiscally-constrained environment.

The technical motivations for each community to be in space are obviously different. UV science needs to be done in space, owing to strong UV absorption in the atmosphere. Direct imaging of exoplanets benefits from space owing to rapidly-varying refraction in the atmosphere which generates focal plane "planet-like" speckles from warped wavefronts.

The attractiveness of a joint UV-exoplanet mission is so great that the two science-based bodies that represent these communities have jointly resolved that it would be highly worthwhile to pursue the required technical advances needed to make such a mission feasible. Specifically, at a joint meeting dedicated to this topic, at Space Telescope Science Institute in April 2011, the Cosmic Origins Program Analysis Group (COPAG) and Exoplanet Exploration Program Analysis Group (ExoPAG) recommended pursuing the study of two types of missions, (a) "A 4-m aperture monolithic telescope with an internal coronagraph of some sort. The coronagraph must be capable of achieving a contrast ratio of $10^{-10}$ or better in order to find exoEarths.", and (b) "An 8-m aperture segmented telescope that relies on an external occulter to achieve the high contrast needed to find an exoEarth.". The meeting was described in a Nature news item[1].

This paper reports a small step toward the goal of a joint UV-exoplanet mission, by addressing the problem of developing a mirror coating that would serve both communities.

## 2. COATING CAPABILITIES AND REQUIREMENTS

Ultraviolet astronomy science requires good mirror reflectivity in the vacuum ultraviolet (VUV, 100 to 200 nm), far ultraviolet (FUV, 122 to 200 nm), middle ultraviolet (MUV, 200 to 300 nm), and near ultraviolet (NUV, 300 to 400 nm) wavelength ranges. We illustrate the state of the art in two currently operating space missions. Fig. 1 (left) shows the effective area of the Hubble Space Telescope (HST), for which the net efficiency is roughly 0.04 percent in the bottom (100 to 110 nm) of its VUV channel. Fig. 1 (right) shows the effective area of the GALEX mission, for which the net efficiency is on the order of 1 percent at the bottom (130 to 170 nm) of its FUV channel.

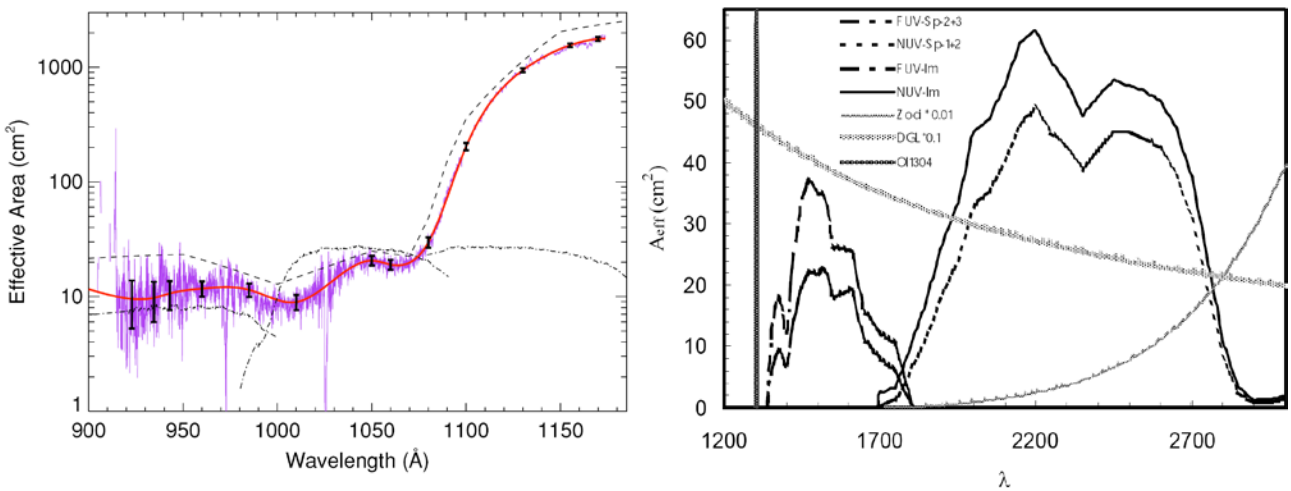


Figure 1. Current capability in UV coating technology for space missions. (left) The effective area of HST, centered on the VUV range, is about 17 $cm^2$ in the 100-110 nm region, for an efficiency of about 0.04 percent (adapted from McCandliss[2]). (right) The effective area of the GALEX telescope, the product of 3 reflections, 1 filter per FUV or NUV channel, and the detector response, all divided by the geometric collecting area of about 1570 $cm^2$, gives about 15 $cm^2$ effective area in the 130-170 nm range, which corresponds to an overall efficiency of about 1 percent (adapted from Martin[3]).

Clearly, UV astronomy would benefit tremendously if telescope efficiency could be increased at short wavelengths. The limiting factor is mirror coatings, as seen in Fig. 2 where we show the theoretical reflectivity of aluminum overcoated with a half-wave of LiF or $MgF_2$. We use a commercially-available thin-film program for the curves in this paper (http://www.thinfilmcenter.com/essential.html). Our examples use 70 nm of Al, 14 nm of LiF, and 25 nm of $MgF_2$, The geometric thicknesses are from Hunter, Osantowski, and Hass[4], to maximize reflectivity at short wavelengths. (However for a coronagraph application, we expect that a thicker layer, 150 to 200 nm, would be required, to minimize transmission leakage.)

The index of refraction ($n$ - $ik$) files used are called Al(1), LiF(2), and MgF2(3). The LiF(2) data is the same as the LiF(1) data supplied in the package, except for the region from 103 to 119 nm where we used an empirically-smoothed set of $n$-values, to replace the erratic-appearing ones, and we used an ad-hoc set of $k$-values, to fill in for apparently missing small values, using the empirical extrapolation rule $k(\lambda) = 0.12(\lambda\text{-}103)^{-0.6}$, where λ has units of nm, derived by extrapolating $k$-values at nearby shorter wavelengths. The $MgF_2$(3) data is the same as the $MgF_2$(2) data supplied in the package, except for the region 112 to 130 nm where we used an empirically-extrapolated set of k-values, to replace the apparently missing small values, using a similar rule $k(\lambda) = 0.196(\lambda\text{-}112)^{-0.6}$. In both cases the replacement index values result in smoother reflectivity curves that more closely match the measured curves in [4] than do the index values in the package.

For an exoplanet mission using an internal coronagraph in the visible wavelength range, we require that the telescope mirror coatings have three properties: (1) high reflectivity, to maximize the number of photons collected; (2) good uniformity of reflectivity across the pupil, with a point-to-point variation of less than about 0.1% RMS in the spatial frequency range likely of interest, e.g., about 2 to 32 cycles per diameter, the purpose being to minimize diffracted-light speckles in the focal plane to a contrast level (speckle intensity divided by central star intensity) less than $10^{-10}$, similar to the Earth/Sun intensity ratio in the visible; and (3) a small value of phase-shift difference between the s- and p-

polarization components. The purpose of the requirement on small phase shift is the same, to control scattered light near the star; the idea is that a phase shift that varies across the pupil is equivalent to an unwanted up or down shift of the reflecting surface, giving rise to a non-flat wavefront, and consequent speckles. However the numerical limit on this effect has not yet been determined, so at present we merely seek to minimize such an s-p phase shift. We note that in general a contrast of $10^{-10}$ is equivalent to a wavefront smoothness of about $\lambda/10{,}000$ (see, e.g., Traub and Oppenheimer [5]), so it would seem from this requirement that a phase shift of less than *(360 deg.)/10,000 = 0.04* deg RMS would be required, and furthermore this needs to be true over the full wavelength range of the coronagraph. However the speckle intensity from such an s-p shift would be centered close to the star, and might not interfere with a search for exoplanets at a sky angle of, say, $3\lambda/D$ and greater, where D is the diameter of the telescope pupil. For present purposes, we merely seek to find phase shifts in what appears to be a practical range of about 1 degree or less, and leave a detailed specification for a subsequent investigation. We note that several specific examples of coating designs have been evaluated for s-p phase shift and applied to an example coronagraph by Balasubramanian et al. [10], who showed that contrasts better than (i.e., lower than) the Earth/Sun target value of $C = 10^{-10}$ were obtained with s-p phase shifts of a few degrees, so this appears to be a practical value from the point of view of coating design and resulting coronagraph contrast values.

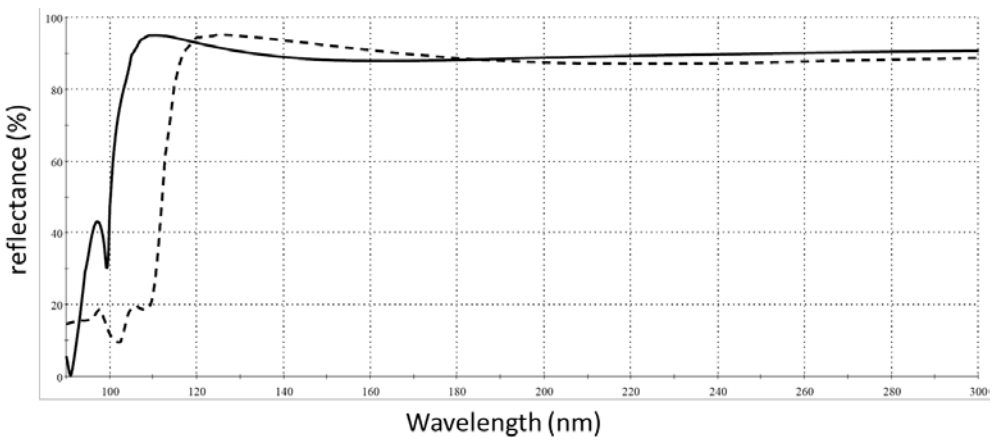


Figure 2. Theoretical reflectance of aluminum overcoated with 14 nm of LiF (solid curve) or 25 nm or $MgF_2$ (dashed curve. The sharp reflectance cutoffs are caused by a strong absorption in LiF in the 94 to 99 nm (full-width at half-maximum) region, and by a similar absorption in $MgF_2$ in the 102 to 110 nm (FWHM) region. The LiF database has $k = 0$ from 119 to 5300 nm, and the $MgF_2$ database has $k = 0$ from 140 to 6250 nm, so we expect no absorption effects from these overcoat materials in these ranges, from the FUV through the mid-thermal infrared for LiF, and through the MUV through the mid-thermal infrared for $MgF_2$.

For comparison with the ideal requirements, we show in Fig. 3 the same reflectivity curves over the full range VUV to near-infrared (here taken to be the 1100 nm cutoff wavelength of Si-based CCD detectors), for the same cases of LiF and $MgF_2$ overcoats on aluminum. The well-known dip in reflectivity from aluminum, at about 700 to 950 nm, is prominent here, independent of the chosen overcoat materials. Overall the single-mirror reflectivity of about 90% is respectably high, but not as high as we might wish. There is certainly room for improvement concerning this parameter, as shown, for example, by Balasubramanian et al. [6], who found coating designs with 3 layers of dielectric over silver, giving high reflectivity (~98%) in the visible, as well as small phase shifts; however silver absorbs strongly in the UV so it is not a candidate for the type of coatings we are seeking in this paper.

Calculated s-p phase shifts for our two prototype coatings are shown in Fig. 4, where we see that the effective shifts in the visible range are on the order of about 1 deg, recognizing that, by convention, 180 deg. is the shift for normal incidence. This shows that these simple coatings are roughly equivalent to those found for silver mirrors [6], and may be acceptable for an exoplanet coronagraph, given the caveats mentioned above, namely that we do not yet have a well-defined requirement for this parameter.

In the following sections, we describe our experiments to produce mirror coatings using atomic layer deposition (ALD), a technique that holds promise for smooth, dense coatings that can be built up at a rate of about one atomic layer per coating cycle, using almost any atom in the periodic table. We see 3 valuable properties of ALD: (1) the coatings are compact, with essentially no voids or column-like structures; (2) the coating thickness is uniform over any shape of substrate; and (3) almost any atomic species can be used.

For our application, these correspondingly translate to (1) the possibility of a dense LiF overcoat that can be used in the open air, where if the LiF is applied in a dense (non-porous) layer, similar to the density of a LiF crystal, which is not hygroscopic, it will be able to block water vapor and oxygen from penetrating to the underlying aluminum, where it creates an opaque $Al_2O_3$ layer; (2) the possibility of coating a very large mirror in a realistically modest size vacuum chamber, since the chamber need be only slightly larger in all dimensions than the mirror itself; and (3) the possibility of developing new kinds of metal and dielectric layer compositions, with hitherto unavailable index of refraction values, at the level of one atomic layer at a time, giving the designer a greater range of control over reflectivity and phase shift than with conventional techniques.

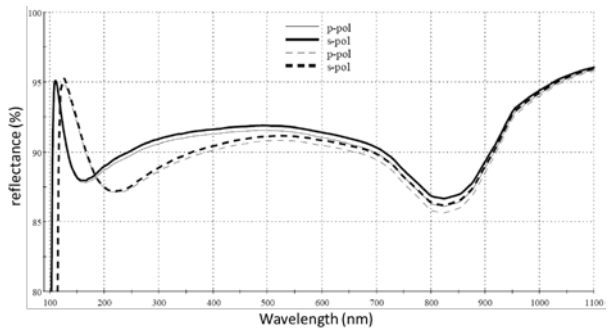


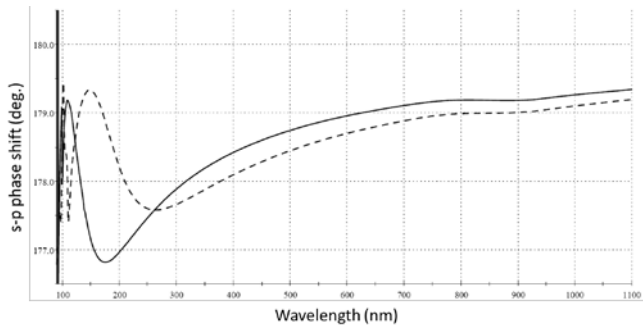


Figure 3 (left). Reflectance of LiF (solid) and $MgF_2$ (dashed) over aluminum, as in Fig. 2, but for s- and p-polarization components, at an angle of incidence of 12 deg., corresponding to the maximum angle of incidence at the edge of a fast, on-axis primary mirror (f# = 1.2). Figure 4 (right). Phase shift difference between s- and p-polarized components of an incident wave, reflecting at an angle of incidence of 12 deg., at a mirror having LiF (solid) and $MgF_2$ (dashed) over aluminum. By convention, 180 deg. corresponds to the shift at normal incidence, so the actual shifts shown here, with respect to normal incidence, at 500 nm for example, are about 1.2 deg for the LiF case, and 1.5 deg. for $MgF_2$.

## 3. ALD: PROCESS AND TECHNIQUE

Atomic layer deposition (ALD) is a cyclical deposition process that utilizes sequential surface reactions to grow thin films one monolayer at a time. A typical ALD process follows the general path sketched in Fig. 5.

A metallic precursor is introduced in a vacuum chamber where it is allowed to react with sites on a substrate of interest, leaving behind a single monolayer of the precursor molecule. The reaction stops once all the sites on the substrate are consumed. Once this occurs, excess metallic precursor is purged from the vacuum chamber either using an inert gas stream or by evacuating the chamber with a pump. When this purge step is complete, a second precursor or reactant is introduced. The second molecule or species reacts with the monolayer that was left behind after the first step in the ALD process to produce the film of interest. When this reaction is complete, the second precursor is purged from the vacuum chamber or pumped out. The final result is approximately one monolayer of the thin film of interest. This Precursor 1/Purge/Precursor 2/purge process can be repeated as many times as desired until the desired film thickness is achieved.

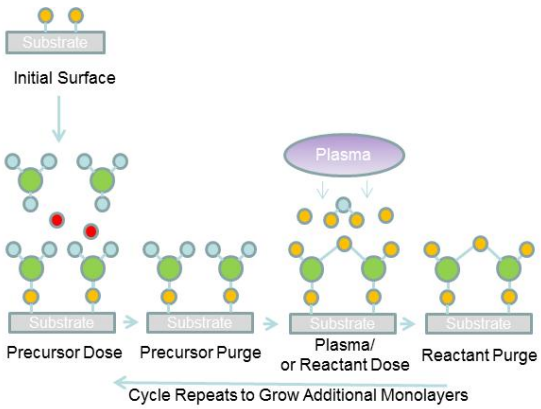


Figure 5: Steps in atomic layer deposition (ALD) processes.

When this mirror coatings study was begun, two ALD processes were selected from the literature, one for the deposition of aluminum thin films [7] and a second for the deposition of magnesium fluoride [8]. However, this magnesium fluoride process was found to be exceedingly difficult to use. The compound "tetramethylheptanedionato magnesium" [$Mg(TMHD)_2$] has a relatively low vapor pressure. Therefore, the material could not be reliably introduced into the deposition chamber to carry out the $MgF_2$ ALD process. For this reason, an alternative deposition chemistry was developed using bisethylcyclopentadienyl magnesium [$Mg(EtCp)_2$] and hydrogen fluoride [HF]. The authors believe that this is the first use of these two molecules to produce $MgF_2$ via ALD. This new alternative pathway to $MgF_2$ was found to be significantly more robust than the reactions published in the literature, and therefore was employed throughout the rest of the work described here. These three reactions are shown in the table below:

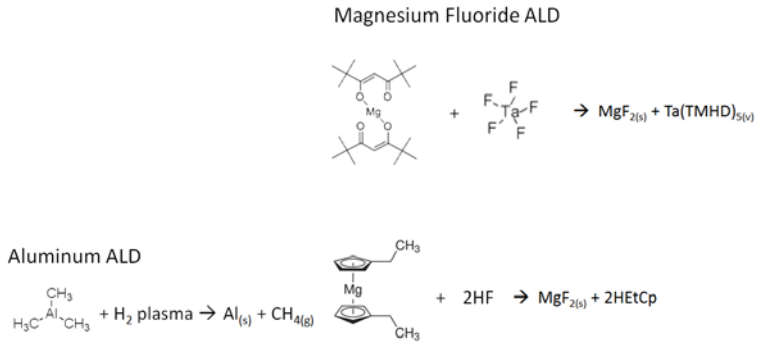


Table 1: ALD reactions for deposition of aluminum (left) and magnesium fluoride (right, 2 different techniques), where (s), (g), and (v) indicate the solid, gas, and vapor phases, respectively. XXXXX FIX FIGURE

All depositions were carried out at 250°C. Thickness calibrations were carried out on silicon substrates using ellipsometry that were subsequently verified by transmission electron microscopy (TEM). Polished glass and silicon carbide substrates were utilized to fabricate mirrors. The reflectivity of these coatings was characterized by a Cary UV-VIS spectrometer at an angle of either 8 or 45 degrees. All measurements were made in reference to an uncoated aluminum mirror inside the instrument. In some experiments, an additional aluminum mirror, fabricated by the authors using e-beam evaporation, was also measured as a secondary standard.

In order to simplify the interpretation of the data, separate depositions of $MgF_2$ were made on substrates coated by e-beam evaporated aluminum rather than by ALD aluminum. This was done to minimize the potential confounding

effects of carrying out two different chemical reactions within the same deposition chamber. As with the ALD aluminum experiments, mirror coatings were made onto polished glass and silicon carbide substrates.

As the depositions on e-beam evaporated aluminum required exposure of the aluminum to room air prior to $MgF_2$ deposition (for logistical reasons, we evaporated the Al in a chamber separate from the chamber used for the $MgF_2$ overcoat), additional experiments were carried out to determine the effects of fluorine pretreatments. As aluminum fluoride is thermodynamically favored over aluminum oxide, some of the glass substrates were exposed to xenon difluoride [$XeF_2$] as a possible method to prepare the surface for $MgF_2$ deposition. It was thought that a $XeF_2$ pretreatment might convert the native oxide of the air-exposed aluminum to aluminum fluoride, thereby passivating it until $MgF_2$ could be deposited as an overlayer. This $XeF_2$ method did not work as intended, however, and as will be detailed below, the deposition of ALD $MgF_2$ directly on the e-beam evaporated aluminum gave far superior results.

## 4. PRELIMINARY RESULTS

Figure 6 (at right) shows the reflectivity versus wavelength of glass substrates coated with e-beam evaporated aluminum measured at an angle of 45 degrees. ALD $MgF_2$ coated, $XeF_2$ treated, and uncoated substrates are compared to an uncoated aluminum reference mirror located within the instrument. The reflectivity of bare aluminum at these wavelengths is shown in figure 6 (at left) taken from [9]. It is extremely encouraging that the reflectivity of the ALD $MgF_2$ coated mirror exceeds that of the reference mirror over the entire range of wavelengths measured. The typical absolute reflectivity achieved by the ALD $MgF_2$ coated mirror (which can be calculated by multiplying the bare aluminum curve at left by the relative reflectivity numbers at right) is in excess of 95% over this wavelength range. This is in very near to the theoretical maximum that can be achieved for protected aluminum films at this $MgF_2$ thickness.

This is particularly impressive given the fact that the uncoated EBeam evaporated aluminum mirror has significantly less reflectivity than the instrument reference mirror. This suggests that there is something that the ALD film deposition process does to repair or improve the EBeam aluminum film beyond simple protection. This effect will be the subject of further investigation as this effort progresses.

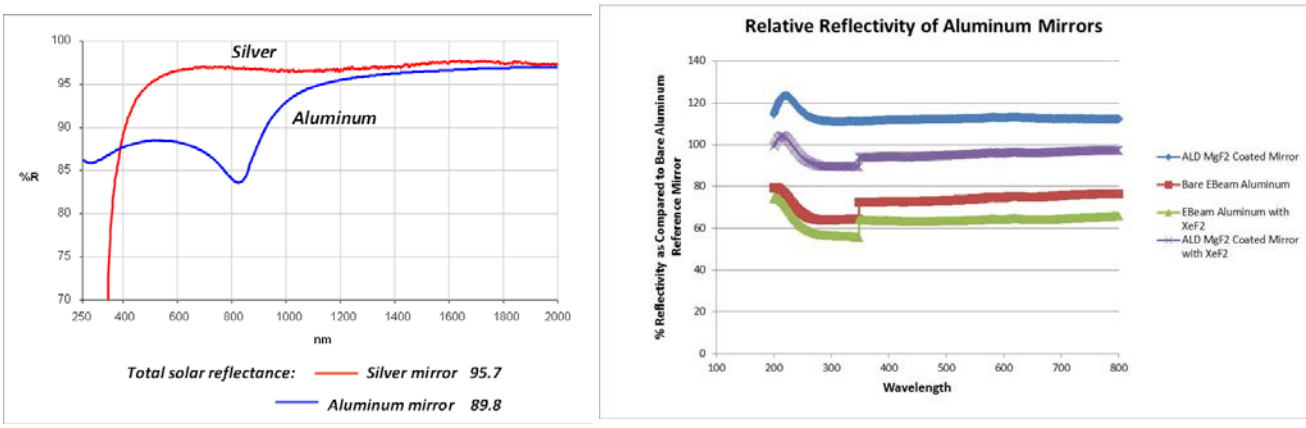


Figure 6. (left) Reflectance spectra of unprotected aluminum and silver mirrors over the NUV to NIR. (right) Relative reflectivity of ALD $MgF_2$ and bare EBeam evaporated aluminum mirror substrates when compared against an internal bare aluminum in a Cary UV-VIS spectrometer.

Conversely, it is clear that the $XeF_2$ treatments negatively impact both the ALD and the bare EBeam evaporated aluminum mirror. Thus, a fluorination pretreatment does not help the mirror surface, but ALD $MgF_2$ significantly improves the overall reflectivity of the substrate.

Figure 7 shows a cross-sectional TEM of an EBeam evaporated aluminum mirror coated by ALD $MgF_2$. Two aspects of this image are particularly promising for the FUV mirror application. First, the film thickness achieved was exactly as was targeted based on the silicon wafer calibrations (20nm). This suggests that the process is a well-behaved ALD reaction and is scalable to large area substrates. But, perhaps more importantly, the film is amorphous as deposited. This is ideal for a thin film moisture barrier, as there are no grain boundaries in the film that would enable diffusion of

oxidizing species. This, at first glance, appears to be superior to the nanocrystalline film morphology that is evident in a commercially available UV enhanced mirror (see Figure 8). However, at the time of this writing, the stability of the reflectivity of an ALD coated mirror has not yet been characterized over a period of time.

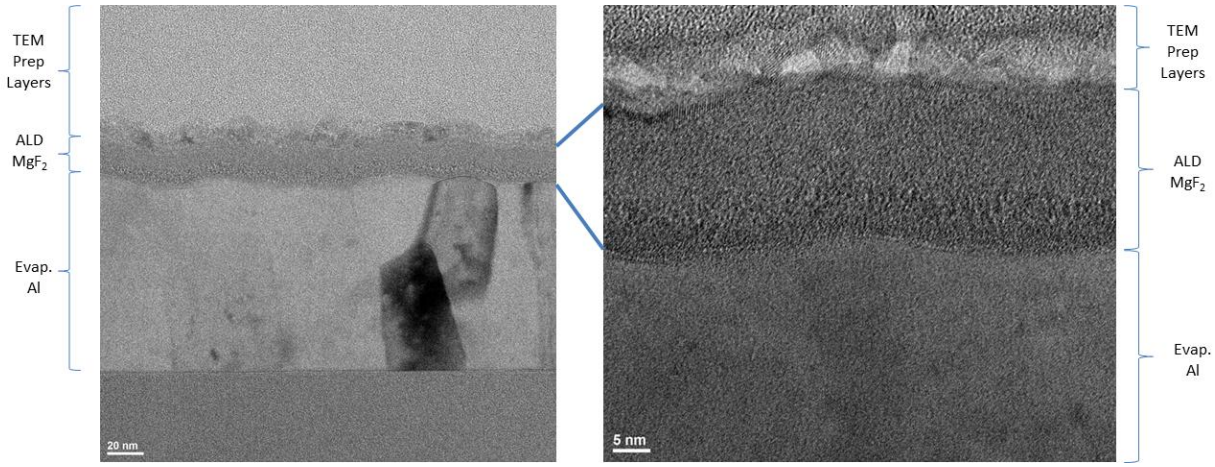


Figure 7: Transmission Electron Micrograph of an ALD $MgF_2$ film as deposited on an EBeam evaporated aluminum film. The base substrate in this case is polished glass.

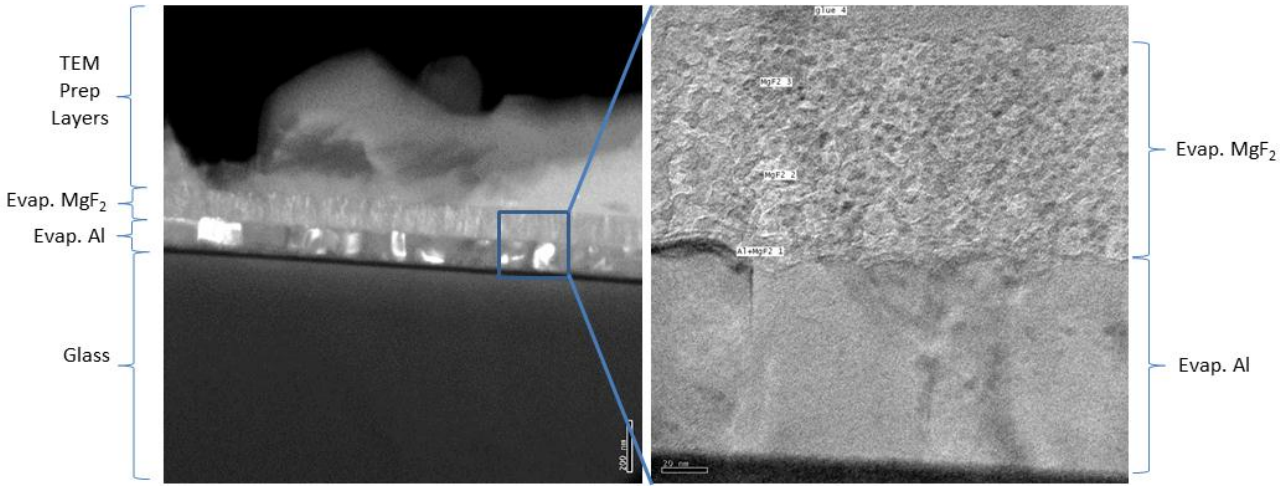


Figure 8: Transmission Electron Micrograph of a commercial-off-the-shelf UV enhanced mirror. The aluminum and $MgF_2$ layers have both been deposited by a physical vapor deposition technique.

## 5. SUMMARY AND PROSPECTS

Based on the initial progress in this study, ALD $MgF_2$ thin films appear to have significant promise as protective coatings for UV-Optical mirrors. Further study is warranted to understand the mechanism of the initial ALD nucleation on the aluminum, as it appears that this is an important factor in mirror performance. In addition, the authors plan to focus on the ALD aluminum process in order to see whether an all-ALD solution for mirror coatings is achievable and desirable.

## 6. ACKNOWLEDGEMENTS

We thank Professor Steven George for helpful discussions regarding $MgF_2$ ALD chemistry, Dr. Matthew Beasley for discussions regarding FUV coatings, Michael C. Lee for his help in the laboratory, and K. (Bala) Balasubramanian for his helpful comment on the manuscript. © 2012 California Institute of Technology. Government sponsorship acknowledged.

* Frank.Greer@jpl.nasa.gov , Shouleh.Nikzad@jpl.nasa.gov , wtraub@jpl.nasa.gov

## REFERENCES

[1] Reich, E. S., "Astronomers mull merger of missions," Nature, 472, 402 (2011).
[2] McCandliss, et al., "Far-ultraviolet sensitivity of the Cosmic Origins Spectrograph," ApJL, 709, L183-L187 (2010).
[3] Martin, C., et al., "The Galaxy Evolution Explorer," Proc. SPIE, 4854, 336-350 (2003).
[4] Hunter, W.R., Osantowski, J.F., and Hass, G., "Reflectance of aluminum overcoated with $MgF_2$ and LiF in the wavelength region from 1600 Angstrom to 300 Angstrom at various angles of incidence," Appl. Opt., 10, 540-544 (1971).
[5] Traub, W.A., and Oppenheimer, B.R., "Direct imaging of exoplanets", pp. 111-156, in Exoplanets, S. Seager, editor, Univ. of Arizona Press (2010).
[6] Balasubramanian, K., Hoppe, D.J., Mouroulis, P.Z., Marchen, L.F., and Shaklan, S.B., "Polarization compensating protective coatings for TPF-coronagraph optics to control contrast degrading cross polarization leakage,", Proc. SPIE, 5905, 59050H-1-59050H-11 (2005).
[7] Aluminum
[8] Magnesium
[9] http://shop.perkinelmer.com/local/kosea/resourcecenter/appnotewebcast/others/focus_solar_energy_properties_architectural_glass.htm
[10] Balasubramanian, K., Shaklan, S., Give'on, A., Cady, E., and Marchen, L., "Deep UV to NIR space telescopes and exoplanet coronagraphs: a trade study on throughput, polarization, mirror coating options and requirements," Proc. SPIE, 8151, 81511G (2011).